Nuclear Engineering and Technology 52 (2020) 2313–2319

Contents lists available at ScienceDirect

Nuclear Engineering and Technology

journal homepage: www.elsevier.com/locate/net

Original Article

Lung tumor segmentation using improved region growing algorithm

Jamshid Soltani-Nabipour [a], Abdollah Khorshidi [b, a, *], Behrooz Noorian [c]

[a] Medical Radiation Engineering Department, Islamic Azad University, Parand Branch, Parand, Iran
[b] School of Paramedical, Gerash University of Medical Sciences, Gerash, Iran
[c] Nuclear Engineering Department, Faculty of Electrical and Computer Engineering, Graduate University of Advanced Technology, Kerman, Iran

ARTICLE INFO

Article history:
Received 24 December 2019
Received in revised form
19 February 2020
Accepted 11 March 2020
Available online 14 March 2020

Keywords:
Region growing algorithm
Automatic thresholding
Tumor boundaries
Accuracy
CT slices

ABSTRACT

The goal of this project is to achieve an accurate segmentation of the pulmonary tumors besides shortening the time and increasing the accuracy. Here, improved region growing (IRG) algorithm is introduced in order to segment the lung tumor with a sufficient accuracy in a shorter time compared to the other basics methods. This comprehensive algorithm was applied on 4 patients CT images and the results of the various steps on segmentation improvement shown 98% accuracy as compared to the basic algorithm. The combination of “multipoint growth start” produced a desirable outcome in accurately bounding the tumor. The proposed algorithm improved tumor identification by less than 13% along with a sufficient percentage of compliance accuracy.

1. Introduction

Radiation therapy is one of the effective ways to treat and counteract the growth and spread of malignant tumors. In order to optimize the treatment, the greatest possible damage to the tumor and the least damage to the healthy tissue are considered. Prior to radiotherapy, the patient's treatment plan must be carefully evaluated to determine the best radiation angle and field dimensions. To do this, it's primarily required to determine the location and size of the tumors. Lung tumors are one of the major types of tumors that cause human deaths. The aim of this study is to identify the pulmonary tumor from CT images. Normally, dividing into specific areas or localization is used as a powerful tool in medical image processing. Its applications are edge and tumor locations detection in the image, determination of the tumor surface, and subsequently it can be mentioned in the post-operative diagnostic stages [1–3]. Prasad et al., 2008 [4] have presented a multi-threshold iterative approach via morphologic operations and polynomial interpolation to determine the curvature of the lung boundary to that of the ribs. Also, Pu et al., 2011 [5] structured a strategy with an implicit function and a radial fitting to remove problematic regions and obtain a closed surface boundary by breaking and then repairing images. Moreover, Rios Velazquez et al., 2012 [6] compared manual and semiautomatic-segmented volumes and overlap fractions in macroscopic lung tumor with limitations in pathological tumor diameter. But optimal surface finding in lung segmentation has been refined by Sun et al., 2013 [7] via a hybrid desktop/virtual reality user interface. In this study, an improved region growing (IRG) algorithm is introduced to increase the accuracy and accelerate the region growth in lung tumor segmentation.

2. Materials and methods

2.1. Basic region growing algorithm

The basic algorithm that we have defined in region growth for 2D images is:

1) The desired slice of a lung containing a tumor is uploaded and called an image.
2) The coordinate of the starting point (pixel) of the growth is determined by the user.
3) The color intensity of this selected point is stored in the base value as *seedval.*
4) Threshold value is considered as *threshval* and by default is 20% gray threshold of the entire image.

$$threshval = .2*\mathrm{graythresh}(image) \quad (1)$$

---

* Corresponding author. School of Paramedical, Gerash University of Medical Sciences, Gerash, Iran.

E-mail addresses: abkhorshidi@yahoo.com, abkhorshidi@chmail.ir (A. Khorshidi).

https://doi.org/10.1016/j.net.2020.03.011

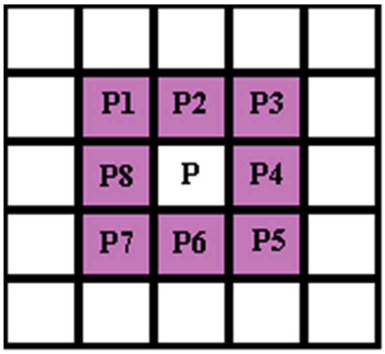

Fig. 1. The 8 neighbor pixels.

5) The coordinates of the first pixel in an array called *points* is saved.
6) The 8 pixels around the starting pixel (neighbor pixels) are considered (Fig. 1). We check that the color intensities of these pixels are within the range of the primary pixel color intensity with a certain accuracy that is the *threshval* value. Each of these points is added to the *points array* provided that the following condition is met:

$$\mathit{seedval} - \mathit{threshval} \le \mathit{pointval} \le \mathit{seedval} + \mathit{threshval} \qquad (2)$$

This is what we call “queuing”.

The above condition is again checked for new neighbor pixels that were in the queue at previous step. According to Fig. 2, this process continues until the pixels are no longer eligible and reach the end of the queue. Now, all pixels in the *points array* that actually form a surface are referred to as the tumor tissue. Also, the outermost pixels are introduced as the tumor boundary, which actually from a curvature.

2.2. Improved region growing (IRG) algorithm

In this research, a new algorithm is proposed to improve the region growth problems and optimize the regional procedure. The IRG method is divided into two phases: pre-processing and main processing for 2D images.

2.2.1. Pre-processing stage

2.2.1.1. Temporary increase in contrast. Increasing the contrast image affects the edges of the tumor, which reduces segmentation accuracy and is considered to have an adverse effect. But proposed algorithm is designed in such a way that at the first stage, the “basic algorithm” is simply to determine the initial tumor range and is not very carefully considered, however at the same time, increasing the contrast speeds the early stage significantly. The increased contrast causes the pulmonary veins to be white spots inside the lung image, and to be mistakenly diagnosed as a tumor and then impair the region growth. Fig. 3 illustrates the effect of contrast enhancement in better visualization of the tumor and removal of the white spots.

2.2.1.2. Specifying the region of the lungs. The purpose of this study is to segment the lung tumor image more accurately, and it is necessary to determine the lung region before performing the “*basic algorithm*”. This has advantages, most importantly in preventing the growth of the region outside the lung in cases where the tumor is attached to the lung wall. Since lung CT images are displayed in black color and the difference in color intensity to the adjacent segments is so large, it is initially possible to apply the “baseline algorithm” to the lung itself to determine the area of the lung. Another approach that seems more reasonable is to perform morphologic operations on the lungs, i.e., to determine the lung area considering the body's anatomy information before performing any tumor identification operations. After finding the lung area, a condition is added to the basic algorithm. This condition considers points that are eligible for the tumor to be within the lung area. Fig. 4 shows an example of specifying the lung area.

2.2.2. Main processing stage

2.2.2.1. Restricting the growth region according to prior information. Normally, changes in tumor growth can be predicted during the treatment process, and therefore the expected maximum size before tumor segmentation is somewhat clear. This can significantly contribute to the improvement of the algorithm. In this case, instead of aligning the entire image in the growth region, we will target a specific region and only that region will be processed. To apply this requirement to the basic algorithm, the user suggests only a maximum diameter for the tumor. Eligible points of the tumor must be at least one diameter away from the starting point of growth. In fact, the process area is limited to a circle in the input image. Fig. 5 illustrates the concept of region restriction in growth procedure.

2.2.2.2. Auto-detecting threshold. In the basic algorithm, the threshold value was set to compare adjacent points by a default of 20% gray level threshold of the whole image. This value is a minimal value obtained empirically for lung tumors. After applying the basic algorithm with this threshold, it is observed that the outer boundaries of the tumor have not been precisely identified. To solve this problem, it is suggested to set a new threshold locally after performing the basic algorithm with a threshold of 20% and identifying the primary tumor's borders. In this way, the threshold is based not on the gray level threshold of the entire image, but on the determination of the gray level threshold in the confined area where the tumor is located. To find this limited area, we suggest determining the center of the tumor's color intensity to circle the

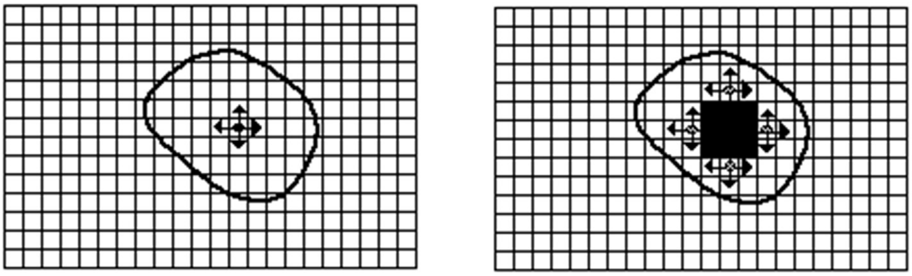

Fig. 2. The procedure of basic region growing algorithm.

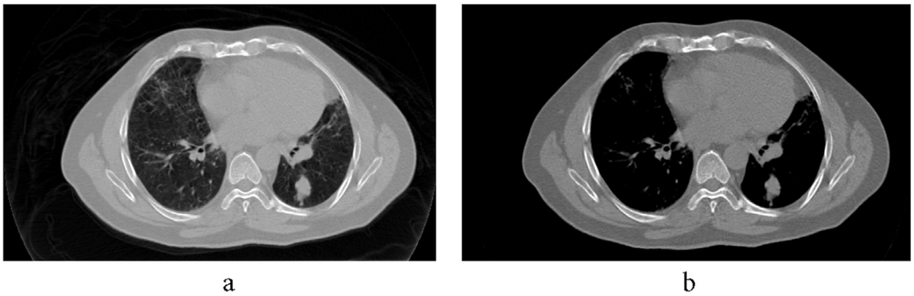
a
b

Fig. 3. Contrast enhancement on tumor visualization: a) without b) with contrast enhancement.

Fig. 4. Specifying the lung area.

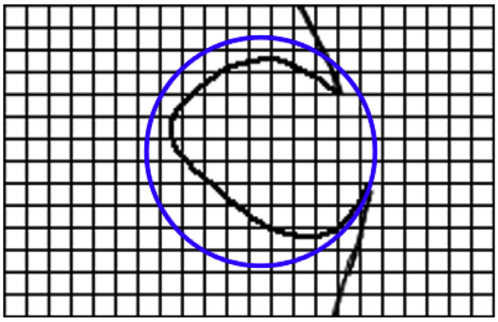

Fig. 5. Growth restriction based on the previous data.

tumor region.

2.2.2.3. Updating comparative value at each step. In all phases of the basic algorithm, the color intensity of the new points is compared with the starting point amount. In order to reduce the error and increase the accuracy, it is recommended to update the region growth of the comparison value in each stage of the algorithm to the mean of the points recognized up to this stage as tumors. Here, the comparative value at each step of algorithm was defined as $seedval_{new} = \frac{1}{n}\sum_{i=1}^{n} I(p_i)$, where I(pi) is the color intensity for point i.

2.2.2.4. Growing from a few points. In order to increase the accuracy of the final result, it is recommended to run the growth algorithm starting from several different points. However, the user still identifies only one starting point, and the other points are logically selected from the entire tumor surface or volume by the following specific mechanism. It also largely ensures the independence of the final result from the starting point. This mechanism would be:

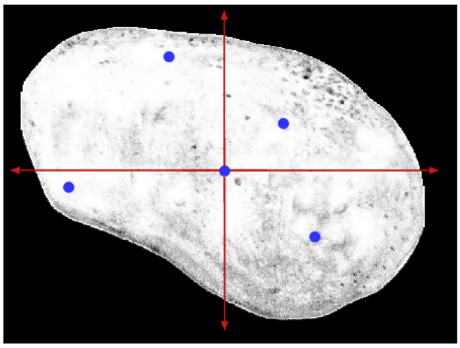

Fig. 6. Starting the growth from different points.

1) After performing the basic algorithm around the point that the user has specified, the geometric center of the tumor is determined as follows,

$$X_{center} = \frac{1}{\#of\ voxels}\sum_{(x,y,z)} x \qquad Y_{center} = \frac{1}{\#of\ voxels}\sum_{(x,y,z)} y \tag{3}$$

2) After determining the geometrical center of the tumor based on the new coordinates, the tumor is divided into 4 zones. A point is randomly chosen from each zone.
3) The basic algorithm starts with 5 points, where one is the center of the tumor and the other is the points set in the previous step.
4) The new tumor will be the result of interpolation between the tumors found in the previous step. Fig. 6 illustrates the visual concept of finding points in region growth.

2.2.2.5. Edge correction. Once the tumor border has been found, it is clear that the edges of the tumor in some cases are not fully covered. To solve this problem, it is suggested that the edges be corrected at the final step. The proposed correction method is to divide the whole full-screen angle into eight parts. Then, we randomly select a point from each region of the main tumor points. Next from each designated point, 3 units diverge from the center of the tumor towards the points that are referred to as the basic algorithm starting points on the edges. In this case, the basic algorithm is implemented with a threshold of 10% instead of 20%.

Table 1
The data used from LCA and DIR labs.

Source lab	Sex and Age	Image size	Image number
DIR	M, 45	512*512*96	1
DIR	M, 65	256*256*112	2
LCA	M, 38	512*512*128	3
LCA	M, –[a]	512*512*120	4

[a] Undetermined.

Applying the growth algorithm to each of these points sets a new region to decide on:

1) If the mean (new region) < mean (main tumor) - 3 SD (main tumor), then the new region is deleted. Which means SD here is a standard deviation.
2) If the area ratio of the new region to the original tumor region is greater than 0.2, then the new region is removed.
3) Otherwise, the new region is added to the main tumor region.

2.2.3. Proposed comprehensive algorithm of region growing

The steps of the comprehensive algorithm are optimally defined as follows:

1) The desired slice of a lung containing a tumor is uploaded and called an image.

2) The contrast of the image is increased.

3) Lung range is determined based on body anatomy. This boundary is called *lungregion.*

4) The coordinate of the starting point (pixel) of the growth algorithm is determined by the user.

5) The color intensity of this point is stored in the base value as *seedval.*

6) The maximum radius expected for a tumor is entered by the user and is called *radiusval.*

7) Threshold value is considered as *threshval* and by default is 20% gray threshold of the whole image (Eq. (1)).

8) The coordinates of the first pixel is stored in an array called *points.*

9) The 8 pixels are considered around the starting pixel (neighboring pixels) and set three conditions for them. **First**, the color intensities of these pixels are with a certain precision in the range of initial color intensity of the starting pixel. **Second**, these points are within the range of the lungs specified in step 3. **Third**, the distance of these points from the starting point is not more than twice the maximum radius expected in step 6. In fact, each of these points is added to the *points array* provided that the following conditions are met,

$$\begin{array}{l} seedval - threshval \leq pointval \leq seedval + threshval \\ point \in lungregion \\ distance\,(seed, point) \leq 2{*}radiusval \end{array} \tag{4}$$

This is called queuing.

10) The *seedval* value is updated to the average of the points that are already in the queue.

$$seedval_{new} = mean\ (I_{points}) \tag{5}$$

11) The step 9 condition for neighboring pixels is again checked by considering new *seedval.*

12) This process continues until the pixels are no longer eligible and reach the end of the queue.

13) All pixels in the points array that actually form a surface are introduced as the primary tumor, and the outermost pixels found are referred to as the primary tumor border which actually form a curve.

14) The color intensity center of the primary tumor is determined and called *iwcogpoint.* Then, the maximum distance from this point to the boundary points specified in the previous step is calculated and called *maxdist.* Now, we consider a circle with *iwcogpoint* center and *maxdist* + 5 radius and call it *targetregion.* The new threshold is 20% of the gray threshold for this region.

$$threshval = .2{*}\mathrm{graythresh}(targetregion) \tag{6}$$

15) The steps 8 to 13 is repeated via the user-defined starting point and the new threshold set in step 14, and then set the tumor boundary.

16) The center of the tumor is determined and called

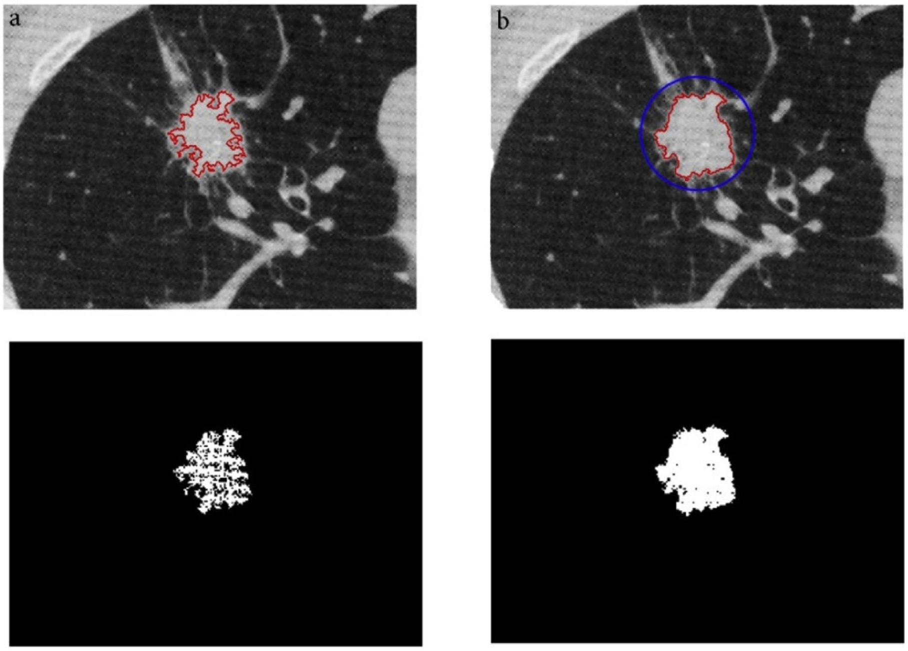

Fig. 7. Finding the threshold limit in a) base and b) automatic modes.

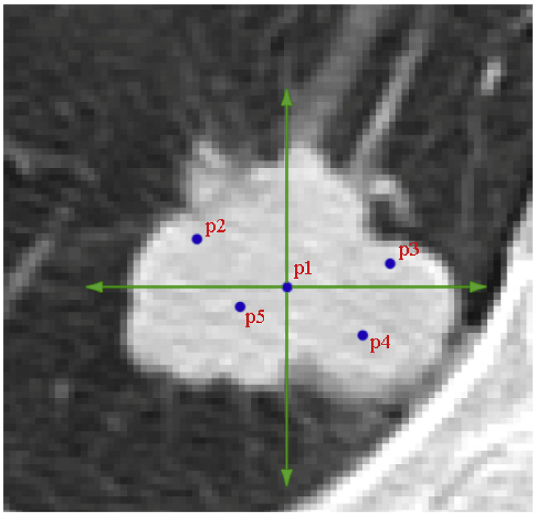

Fig. 8. Selected points in primary tumor to start growing from a few points by the center of p1.

tumorcenter. Now, we divide the tumor into 4 zones according to this center. From each of these zones, one point is randomly selected, and then we have a total of 5 points.

17) The steps 8 to 15 are performed starting from 5 designated points, and then we define 5 boundaries for the tumor. Interpolation between these 5 boundaries introduces the new tumor boundary.

18) The 8 lines are drawing from the tumor center at angles of 0, 45, 90, 270, and 315°, and then the intersections with the tumor boundaries are determined. After that, we are about 3 units away from the border and shall have 8 points for edge correction.

19) Steps 8 to 13 are again performed by these 8 new points and with a threshold of 10%, and divided into 8 grown regions.

20) Each of the 8 new regions is annexed to the main region (step 17) if the following conditions are met:

A) mean (new region) > mean (main tumor) − 3 SD (main tumor)

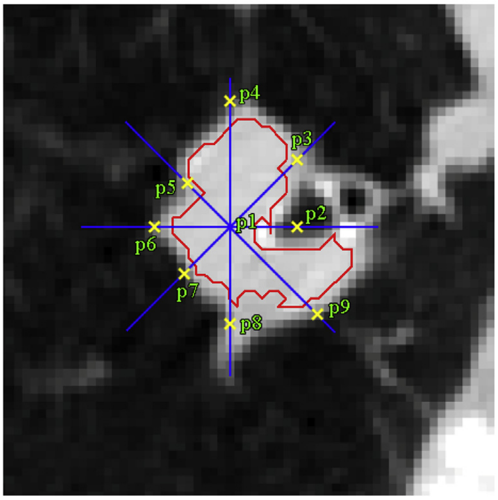

Fig. 10. 9 selected points to correct tumor edges.

B) The ratio of new region to primary tumor is less than 0.2

21) Finally, we reach a surface that is described as a segmented tumor by the “improved region growing” method.

3. Outcomes

In this study, images presented at two valid websites, Lung Cancer Alliance (LCA) [8] and DIR-lab [9] reference sites were used to evaluate the proposed method in lung cancer acquired by CT images. It is sometimes observed that the format of numbers differs from existing data. To integrate the algorithm and the comparability of the results, all numbers were double format and normalized to 0 and 1. Table 1 details the data used in this study.

3.1. Temporary contrast enhancement

At the beginning of the implementation, a contrast enhancement was made for each image. *Imadjust* command was used to

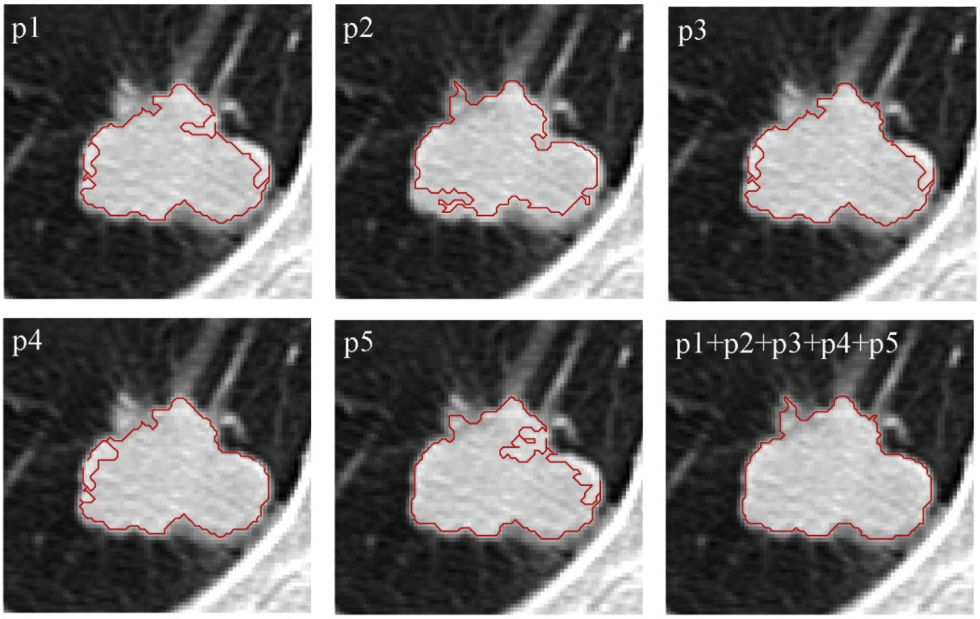

Fig. 9. Growing the region from different points of Fig. 8.

Fig. 11. Implementation of comprehensive region growth algorithm on 2D images.

increase the contrast. Then, restriction on growth algorithm implemented to get better diagnosis. This restriction prevents the area from mistakenly entering the lung wall.

3.2. *Auto-detect threshold*

Fig. 7 demonstrates an example of implementation of the automatic threshold detection method. Fig. 7a relates to a condition where the initial threshold value was 20% of the gray threshold. In this case, the gray threshold was 0.48 and threshold value was 0.096. After the primary tumor was found, the center of tumor color intensity was at (157,146) point of the coordinate. Then, the maximum distance from this center to the tumor border was found to be 34 units and a circle with a radius of 5 units greater than 39 units was drawn around the tumor according to Fig. 7b. In this case, the gray threshold was 0.64 and the threshold value of 20% was 0.128. Subsequently, updating the *comparative value* of color intensity has been implemented at each stage of the algorithm.

Table 3
The result of applying the basic and improved region growing algorithm.

Image number	Basic algorithm CP	Comprehensive algorithm CP
1	65%	93%
2	70%	93%
3	73%	94%
4	84%	98%

3.3. *The outcomes of growth from several points*

Fig. 8 shows the implementation of the growth start from several points. After identifying the initial tumor, the geometrical center of tumor is determined by p1 point. Then, the tumor is divided into 4 parts by the center of p1 and designated p2 to p5 whose positions have been shown in parenthesis.

The growth algorithm continued around each of these 5 selected points, and the result has been separately shown in Fig. 9. The last image shows that the combination of “multipoint growth start”

Table 2
Compliance percentage (CP) derived from the impact of automatically finding the threshold and updating the *comparative value* at each step.

Image number	CP with default threshold of 20%	CP with automatic threshold finding	CP without updating the comparative value at each step	CP with updating the comparative value at each step
1	64%	79%	64%	73%
4	81%	94%	81%	83%

produces a desirable image outcome in bounding the tumor accurately.

3.4. Edge correction and comprehensive algorithm outcomes

After finding the tumor center, 8 points is selected with equal angles at a distance of 3 pixels from the edge of the tumor. In addition to the midpoint, we have a total of 9 points. Fig. 10 shows the selected points for edge correction. The region growth is achieved from these 9 points with a 5% threshold.

Some points of the edges that are the “candidate for growth” have formed the new zone, and the zones that were eligible have been added to the main region. Lastly, the final outcome of the comprehensive algorithm has been illustrated in Fig. 11 as example.

4. Discussion

The accuracy of “specifying the lung area” and “limiting the growth area” cannot be verified by examining the degree of conformity. In fact, these two parts are fundamental reforms because in cases where the tumor is stuck to the wall, failure to perform these two modifications can lead to a major error in the region growing algorithm. Table 2 compares the percentage of compliance in both the “Auto Threshold” and “Default Threshold” modes as well as the threshold percentage with and without updating the “*comparative value*” at each step for two different slices. Both auto-threshold finding and *comparative-value* updating methods have demonstrated a positive effect on the compliance by maximum 15% and 13% raise for image 1 and 4, respectively.

Finally, a comprehensive algorithm covering all previous methods was applied to 4 images. The presented outcomes in Table 3 show that in a variety of images this comprehensive algorithm as compared to the basic algorithm has been able to largely accomplish tumor segmentation with sufficient accuracy. The minimum and maximum CP differences of using these algorithms were 14% and 28% for images 4 and 1, respectively.

Dehmeshki et al. [10] have presented nodule segmentation through fuzzy connectivity map of sphere objects and removing holes from foreground regions to estimate seed-point position and confined volume by 84% acceptance in detection. Also, Keshani et al. [11] have utilized vector machine classifier to detect the nodules and then extract contours via active modeling by 89% performance beside 7.3/scan false positive number. In lung CT images, the region growing method can be combined with other techniques and the threshold value can be determined via color intensity process. In the next study, a default anatomy-based program will be written that find the starting point using intelligent algorithms so that there is no need for the user to specify the starting point.

5. Conclusion

Overall in this research, it is observed that the proposed algorithm has achieved less than 13% improvement in tumor identification by a sufficient compliance percentage on the results accuracy. The implementation of the algorithm as “region growing start from multiple points” beside the “edge correction at the last step” had a major impact on the obtained results. The proposed comprehensive algorithm can be applied to brain tumors and breast cancer by closely matching the color intensity of the tumor and the background tissues and then determining the optimal state.

Declaration of competing interest

The authors declare that they have no known competing financial interests or personal relationships that could have appeared to influence the work reported in this paper.

References

[1] A. Osareh, B. Shadgar, A segmentation method of lung cavities using region aided geometric snakes, J. Med. Syst. 34 (4) (2010) 419–433, https://doi.org/10.1007/s10916-009-9255-z.
[2] J.S. Nabipour, A. Khorshidi, Spectroscopy and optimizing semiconductor detector data under X and γ photons using image processing technique, J. Med. Imag. Radiat. Sci. 49 (2) (2018) 194–200, https://doi.org/10.1016/j.jmir.2018.01.004.
[3] G. Khaleghi, J. Soltani-Nabipour, A. Khorshidi, F. Taheri, Design of band-pass filters by experimental and simulation methods at the range of 100-125 keV of X-ray in fluoroscopy, Int. J. Biosci. Technol. (2019), https://doi.org/10.1504/IJBET.2019.10025733. Accepted.
[4] M.N. Prasad, M.S. Brown, S. Ahmad, F. Abtin, J. Allen, I. da Costa, H.J. Kim, M.F. McNitt-Gray, J.G. Goldin, Automatic segmentation of lung parenchyma in the presence of diseases based on curvature of ribs, Acad. Radiol. 15 (9) (2008) 1173–1180, https://doi.org/10.1016/j.acra.2008.02.004.
[5] J. Pu, D.S. Paik, X. Meng, J.E. Roos, G.D. Rubin, Shape “break-and-repair” strategy and its application to automated medical image segmentation, IEEE Trans. Visual. Comput. Graph. 17 (1) (2011) 115–124, https://doi.org/10.1109/TVCG.2010.56.
[6] E. Rios Velazquez, H.J. Aerts, Y. Gu, D.B. Goldgof, D. De Ruysscher, A. Dekker, R. Korn, R.J. Gillies, P. Lambin, A semiautomatic CT-based ensemble segmentation of lung tumors: comparison with oncologists' delineations and with the surgical specimen, Radiother. Oncol. 105 (2) (2012) 167–173, https://doi.org/10.1016/j.radonc.2012.09.023.
[7] S. Sun, M. Sonka, R.R. Beichel, Lung segmentation refinement based on optimal surface finding utilizing a hybrid desktop/virtual reality user interface, Comput. Med. Imag. Graph. 37 (1) (2013) 15–27, https://doi.org/10.1016/j.compmedimag.2013.01.003.
[8] Lung Cancer Alliance, LCA. Washington, DC. https://lungcanceralliance.org/.
[9] The Deformable Image Registration Lab, DIR-Lab. Winship Cancer Institute, Emory University, Atlanta, GA. https://www.dir-lab.com/.
[10] J. Dehmeshki, H. Amin, M. Valdivieso, X. Ye, Segmentation of pulmonary nodules in thoracic CT scans: a region growing approach, IEEE Trans. Med. Imag. 27 (4) (2008) 467–480, https://doi.org/10.1109/TMI.2007.907555.
[11] M. Keshani, Z. Azimifar, F. Tajeripour, R. Boostani, Lung nodule segmentation and recognition using SVM classifier and active contour modeling: a complete intelligent system, Comput. Biol. Med. 43 (4) (2013) 287–300, https://doi.org/10.1016/j.compbiomed.2012.12.004.